

# Second-Order Divided-Difference Filter Using a Generalized Complex-Step Approximation

Kok-Lam Lai\* and John L. Crassidis†

*University at Buffalo, State University of New York, Amherst, NY 14260-4400*

This paper presents a framework for the second-order divided-difference filter using a generalized complex-step derivative approximation. For first derivatives the complex-step approach does not suffer subtraction cancellation errors as in standard numerical finite-difference approaches. Therefore, since an arbitrarily small step size can be chosen, the complex-step method can achieve near analytical accuracy. However, for second derivatives straight implementation of the complex-step approach does suffer from roundoff errors. Therefore, an arbitrarily small step size cannot be chosen. Previous work expanded upon the standard complex-step approach to provide a wider range of accuracy for both the first and second derivative approximations. The new extensions can allow the use of one step size to provide optimal accuracy for both derivative approximations, which are used in the divided-difference filter in order to improve its accuracy. Simulation results are provided to show the performance of the new complex-step approximations on the divided-difference filter.

## I. Introduction

Filtering algorithms, such as the extended Kalman filter<sup>1</sup> (EKF), the Unscented Kalman filter<sup>2</sup> (UKF) and Particle filters<sup>3,4</sup> (PFs), are commonly used to both estimate unmeasurable states and filter noisy measurements. The EKF and UKF assume that the process noise and measurement noise are represented by zero-mean Gaussian white-noise processes. Even if this is true, both filters only provide approximate solutions when the state and/or measurement models are nonlinear, since the posterior density function is most often non-Gaussian. The EKF typically works well only in the region where the first-order Taylor-series linearization adequately approximates the non-Gaussian probability density function (pdf). The UKF falls into the category of filters that do not require linearizations of the state dynamics propagation and measurement model equations.<sup>5</sup> Reference 6 further classifies these filters collectively as “Linear Regression Kalman filters,” since they all fall into the category of filters that linearize the statistics of the nonlinear models instead of the nonlinear models themselves. While finding the Jacobian and Hessian matrices are not needed, these filters attempt to capture the statistics of transformations via finite-difference equations. However, these filters still fall into the general category of the Kalman filter that updates the propagated states linearly as a function of the difference between estimated measurements and actual measurements.

The UKF works on the premise that with a fixed number of parameters it should be easier to approximate a Gaussian distribution than to approximate an arbitrary nonlinear function. This in essence can provide higher-order moments for the computation of the posterior function without the need to calculate jacobian matrices as required in the EKF. Still, the standard form of the EKF has remained the most popular method for nonlinear estimation to this day, and other designs are investigated only when the performance of this standard form is not sufficient. The Divided-Difference Filter (DDF) uses divided-difference approximations of derivatives based on Stirling’s interpolation formula.<sup>7</sup> In comparison with the EKF, the DDF results in a similar mean, but a different posterior covariance. The DDF uses techniques based on similar principles to those of the UKF. As stated in Ref. 8, the DDF and the UKF simply retain a different subset of cross-terms in the higher-order expansions. The DDF has a smaller absolute error in the fourth-order term and also

---

\*Ph.D., Department of Mechanical & Aerospace Engineering. Email: klai2@buffalo.edu. Student Member AIAA.

†Associate Professor, Department of Mechanical & Aerospace Engineering. Email: johnc@eng.buffalo.edu. Associate Fellow AIAA.

guarantees positive semi-definiteness of the posterior covariance, while the UKF may result in a non-positive semi-definite covariance. The second-order Divided-Difference (DD2) filter from Ref. 5 is a more generalized version of the UKF that offers the same mean estimation accuracy. However, the covariance estimation is more accurate in the DD2 filter from more accurate treatment of the Gaussian statistics. Also, the DD2 filter operates at the square-root level.

This paper deals with complex-step approximations of derivatives for use in the DDF. Using complex numbers for computational purposes is often intentionally avoided because the nonintuitive nature of this domain. However, this perception should not handicap our ability to seek better solutions to the problems associated with traditional (real-valued) finite-difference approaches. Many physical world phenomena actually have their roots in the complex domain.<sup>9</sup> As an aside we note that some interesting historical notes on the discovery and acceptance of the complex variable can also be found in this reference. A brief introduction of complex variable could be found on Ref. 10, pp. 1108-1109. The complex-step derivative approximation (CSDA) can be used to determine first derivatives in a relatively easy way, while providing near analytic accuracy. Early work on obtaining derivatives via a complex-step approximation in order to improve overall accuracy is shown by Lyness and Moler,<sup>11</sup> as well as Lyness.<sup>9</sup> Various recent papers reintroduce the complex-step approach to the engineering community.<sup>12-16</sup> The advantages of the complex-step approximation approach over a standard finite difference include: 1) the Jacobian approximation is not subject to subtractive cancelations inherent in roundoff errors, 2) it can be used on discontinuous functions, and 3) it is easy to implement in a black-box manner, thereby making it applicable to general nonlinear functions. In this paper, the first and second-order finite differences used in derivation of the DD2 filter will be replaced with complex-step derivative approximations and thus generalizes it to the complex domain.

The organization of this paper is as follows. First, the complex-step approximation to the derivative is reviewed for both the first and second-order derivatives. Then, the generalized complex-step approximation is summarized for both the scalar and vector cases. Next, the approximations are used to approximate the mean and covariance of a stochastic function, followed by the second-order approximation. Then, the second-order complex divided-difference filter is shown. Finally, simulation comparisons are made between the standard DD2 and new CSDA filters.

## II. Complex-Step Approximation to the Derivative

In this section the complex-step approximation is shown. First, the derivative approximation of a scalar variable is summarized, followed by an extension to the second derivative. Then, approximations for multi-variable functions are presented for the Jacobian and Hessian matrices. Numerical finite difference approximations for any order derivative can be obtained by Cauchy's integral formula<sup>17</sup>

$$f^{(n)}(z) = \frac{n!}{2\pi i} \int_{\Gamma} \frac{f(\xi)}{(\xi - z)^{n+1}} d\xi \quad (1)$$

This function can be approximated by

$$f^{(n)}(z) \approx \frac{n!}{mh} \sum_{j=0}^{m-1} \frac{f\left(z + h e^{i\frac{2\pi j}{m}}\right)}{e^{i\frac{2\pi jn}{m}}} \quad (2)$$

where  $h$  is the step size and  $i$  is the imaginary unit,  $\sqrt{-1}$ . For example, when  $n = 1$ ,  $m = 2$

$$f'(z) = \frac{1}{2h} [f(z+h) - f(z-h)] \quad (3)$$

We can see that this formula involves a subtraction that would introduce near cancelation errors when the step size becomes too small.

### II.A. First Derivative

The derivation of the complex-step derivative approximation is accomplished by approximating a nonlinear function with a complex variable using a Taylor's series expansion:<sup>15</sup>

$$f(x + ih) = f(x) + ihf'(x) - \frac{h^2}{2!}f''(x) - i\frac{h^3}{3!}f^{(3)}(x) + \frac{h^4}{4!}f^{(4)}(x) + \dots \quad (4)$$

Taking only the imaginary parts of both sides gives

$$\Im\{f(x + ih)\} = hf'(x) - \frac{h^3}{3!}f^{(3)}(x) + \dots \quad (5)$$

Dividing by  $h$  and rearranging yields

$$f'(x) = \frac{\Im\{f(x + ih)\}}{h} + \frac{h^2}{3!}f^{(3)}(x) + \dots \quad (6)$$

$O(h^2) \approx 0$

Terms with order  $h^2$  or higher can be ignored since the interval  $h$  can be chosen up to machine precision. Thus, to within first-order the complex-step derivative approximation is given by

$$f'(x) = \frac{\Im\{f(x + ih)\}}{h} \quad , \quad E_{\text{trunc}}(h) = \frac{h^2}{6}f^{(3)}(x) \quad (7)$$

where  $E_{\text{trunc}}(h)$  denotes the truncation error. Note that this solution is not a function of differences, which ultimately provides better accuracy than a standard finite difference.

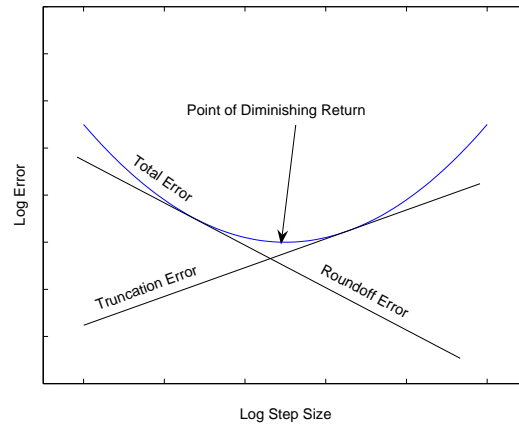


Figure 1. Finite Difference Error Versus Step Size

## II.B. Second Derivative

In order to derive a second derivative approximation, the real components of Eq. (4) are taken, which gives

$$\Re\left\{\frac{h^2}{2!}f''(x)\right\} = f(x) - \Re\{f(x + ih)\} + \frac{h^4}{4!}f^{(4)}(x) + \dots \quad (8)$$

Solving for  $f''(x)$  yields

$$f''(x) = \frac{2!}{h^2}\left[f(x) - \Re\{f(x + ih)\}\right] + \frac{2!h^2}{4!}f^{(4)}(x) + \dots \quad (9)$$

Analogous to the approach shown before, we truncate up to the second-order approximation to obtain

$$f''(x) = \frac{2}{h^2}\left[f(x) - \Re\{f(x + ih)\}\right] \quad , \quad E_{\text{trunc}}(h) = \frac{h^2}{12}f^{(4)}(x) \quad (10)$$

As with Cauchy's formula, we can see that this formula involves a subtraction that may introduce machine cancelation errors when the step size is too small. Hence, this approach is subject to roundoff errors for small step sizes since difference errors arise, as shown by the classic plot in Figure 1. As the step size increases the accuracy decreases due to truncation errors associated with not adequately approximating the true slope at the point of interest. Decreasing the step size increases the accuracy, but only to an "optimum" point. Any further decrease results in a degradation of the accuracy due to roundoff errors. Hence, a tradeoff between truncation errors and roundoff exists. In fact, through numerous simulations, the complex-step second-derivative approximation is markedly *worse* than a standard finite-difference approach.<sup>18</sup>

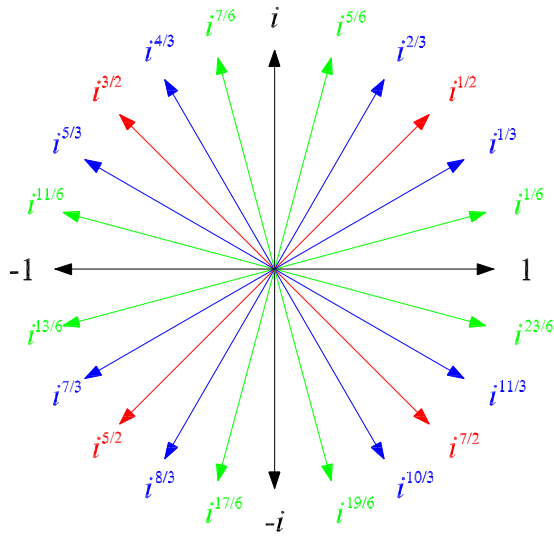


Figure 2. Various Complex Numbers

### III. Generalized Complex-Step Approximations

#### III.A. Scalar Case

Reference 18 presents a generalization of the complex-step approach, which showed better performance characteristics in the first and second-order approximations than the standard complex-step derivatives. The basic idea involves a linearization about a general complex number, rather than  $i$  alone. The step size for the difference and average operators are augmented with a unity magnitude complex number:

$$\delta f(x) \equiv f\left(x + \frac{1}{2}e^{\theta i}h\right) - f\left(x - \frac{1}{2}e^{\theta i}h\right) \quad (11a)$$

$$\mu f(x) \equiv \frac{1}{2} \left[ f\left(x + \frac{1}{2}e^{\theta i}h\right) + f\left(x - \frac{1}{2}e^{\theta i}h\right) \right] \quad (11b)$$

where  $\theta$  is the associated “angle” of departure from the positive real axis. Figure 2 shows the unity magnitude complex number raised to various rational number powers with common denominator of 6, i.e. multiple of  $15^\circ$ . Let’s take a moment and revisit the Taylor series nominally at  $\bar{x}$ :

$$f(x) = f(\bar{x}) + f'(\bar{x})(x - \bar{x}) + \frac{1}{2!}f''(\bar{x})(x - \bar{x})^2 + \frac{1}{3!}f^{(3)}(\bar{x})(x - \bar{x})^3 \dots \quad (12)$$

and a Taylor series with step size of  $+e^{\theta i}h$  and  $-e^{\theta i}h$ :

$$\begin{aligned} f(x) = f(\bar{x} + e^{\theta i}h) &= f(\bar{x}) + f'(\bar{x})(e^{\theta i}h) + \frac{1}{2!}f''(\bar{x})(e^{\theta i}h)^2 \\ &+ \frac{1}{3!}f^{(3)}(\bar{x})(e^{\theta i}h)^3 + \frac{1}{4!}f^{(4)}(\bar{x})(e^{\theta i}h)^4 + \dots \end{aligned} \quad (13a)$$

$$\begin{aligned} f(x) = f(\bar{x} - e^{\theta i}h) &= f(\bar{x}) - f'(\bar{x})(e^{\theta i}h) + \frac{1}{2!}f''(\bar{x})(e^{\theta i}h)^2 \\ &- \frac{1}{3!}f^{(3)}(\bar{x})(e^{\theta i}h)^3 + \frac{1}{4!}f^{(4)}(\bar{x})(e^{\theta i}h)^4 + \dots \end{aligned} \quad (13b)$$

A Taylor series expansion evaluates the derivative information of an analytical function at a precise point and assumes these derivatives to remain valid around the vicinity of this point. For highly nonlinear functions, the derivative calculations deviate quickly from the nominal point. Therefore, derivative information with uniform performance across a region of interest should be used. This is achieved with derivatives derived by using interpolation. Another advantage is that interpolations generally require only function evaluations

and not analytical derivations. The Stirling interpolation<sup>19</sup> is chosen to obtain the derivation information. With the Stirling interpolation, an approximation of a nonlinear function can be expressed as

$$\begin{aligned}
f(x) &= f(\bar{x} + e^{\theta i} p h) \\
&= f(\bar{x}) + p \mu \delta f(\bar{x}) + \frac{1}{2!} p^2 \delta^2 f(\bar{x}) + \binom{p+1}{3} \mu \delta^3 f(\bar{x}) + \frac{1}{4!} p^2 (p^2 - 1) \delta^4 \\
&\quad + \binom{p+2}{5} \mu \delta^5 f(\bar{x}) + \dots
\end{aligned} \tag{14}$$

Generally,  $-1 < p < 1$  as for interpolation within the region of interest, between  $-h$  and  $+h$ . Concentrating only on the first two derivative expansions gives

$$f(x) \approx f(\bar{x}) + f'_{CSDA}(\bar{x})(x - \bar{x}) + \frac{1}{2!} f''_{CSDA}(\bar{x})(x - \bar{x})^2 \tag{15}$$

where  $f'_{CSDA}(\bar{x})$  and  $f''_{CSDA}(\bar{x})$  are the first and second complex-step derivative approximations without the truncation error:

$$f'_{CSDA}(x) = \frac{f(x + e^{i\theta} h) - f(x - e^{i\theta} h)}{2e^{i\theta} h} \tag{16a}$$

$$f''_{CSDA}(x) = \frac{f(x + e^{i\theta} h) - 2f(x) + f(x - e^{i\theta} h)}{(e^{i\theta} h)^2} \tag{16b}$$

Equation (15) is basically a Taylor series with derivatives replaced with CSDAs. Assuming  $f$  is analytic, substituting Eqs. (13) into Eqs. (16) for Eq. (15) yields

$$\begin{aligned}
&f(\bar{x}) + f'_{CSDA}(\bar{x})(x - \bar{x}) + \frac{1}{2!} f''_{CSDA}(\bar{x})(x - \bar{x})^2 \\
&= f(\bar{x}) + f'(\bar{x})(x - \bar{x}) + \frac{1}{2!} f''(\bar{x})(x - \bar{x})^2 \\
&\quad + \left[ \frac{1}{3!} f^{(3)}(\bar{x})(e^{\theta i} h)^2 + \frac{1}{5!} f^{(5)}(\bar{x})(e^{\theta i} h)^4 + \dots \right] (x - \bar{x}) \\
&\quad + \left[ \frac{1}{4!} f^{(4)}(\bar{x})(e^{\theta i} h)^2 + \frac{1}{6!} f^{(6)}(\bar{x})(e^{\theta i} h)^4 + \dots \right] (x - \bar{x})^2
\end{aligned} \tag{17}$$

The first three terms on the right-hand-side of the equation are the first three terms of the Taylor series. The choice of  $h$  has an influence only on the “remainder” terms and the optimal choice of  $h$  is explored in Ref. 5 to be  $h^2 = 3$  for a Gaussian distribution. Another variable to be manipulated to our advantage is the  $\theta$  value, which is related to the power of an imaginary number.

### III.B. Vector Case

The scalar analysis is now extended to the multi-variable case, with  $\mathbf{x} \in \mathbb{R}^n$ . The two Stirling operators in vector forms are simply

$$\delta_p \mathbf{f}(\mathbf{x}) \equiv \mathbf{f} \left( \mathbf{x} + \frac{1}{2} e^{\theta i} h \boldsymbol{\varepsilon}_p \right) - \mathbf{f} \left( \mathbf{x} - \frac{1}{2} e^{\theta i} h \boldsymbol{\varepsilon}_p \right), \tag{18a}$$

$$\mu_p \mathbf{f}(\mathbf{x}) \equiv \frac{1}{2} \left[ \mathbf{f} \left( \mathbf{x} + \frac{1}{2} e^{\theta i} h \boldsymbol{\varepsilon}_p \right) + \mathbf{f} \left( \mathbf{x} - \frac{1}{2} e^{\theta i} h \boldsymbol{\varepsilon}_p \right) \right], \tag{18b}$$

where the subscript  $p$  emphasizes it is the  $p^{\text{th}}$  “partial” operator with  $\boldsymbol{\varepsilon}_p$  being the  $p^{\text{th}}$  column of a  $p \times p$  identity matrix (the  $p^{\text{th}}$  basis vector).

Let  $\mathbf{y} = \mathbf{f}(\mathbf{x})$  denote a nonlinear vector transformation. Its Taylor series can be expressed as

$$\begin{aligned}
\mathbf{y} &= \mathbf{f}(\bar{\mathbf{x}} + \Delta \mathbf{x}) = \sum_{p=0}^{\infty} \frac{1}{p!} D_{\Delta \mathbf{x}}^p \mathbf{f} \\
&= \mathbf{f}(\bar{\mathbf{x}}) + D_{\Delta \mathbf{x}} \mathbf{f} + \frac{1}{2!} D_{\delta \mathbf{x}}^2 \mathbf{f} + \frac{1}{3!} D_{\delta \mathbf{x}}^3 \mathbf{f} + \dots
\end{aligned} \tag{19}$$

where

$$D_{\Delta x}^p \mathbf{f} = \left[ \Delta x_1 \frac{\partial}{\partial x_1} + \Delta x_2 \frac{\partial}{\partial x_2} + \cdots + \Delta x_n \frac{\partial}{\partial x_n} \right]^p \mathbf{f}(\mathbf{x}) \Big|_{\mathbf{x}=\bar{\mathbf{x}}} \quad (20)$$

The first two operators are simply

$$D_{\Delta x} \mathbf{f} = \left[ \sum_{p=1}^n \Delta x_p \frac{\partial}{\partial x_p} \right] \mathbf{f}(\mathbf{x}) \Big|_{\mathbf{x}=\bar{\mathbf{x}}} \quad (21a)$$

$$D_{\Delta x}^2 \mathbf{f} = \left[ \sum_{p=1}^n \sum_{q=1}^n \Delta x_p \Delta x_q \frac{\partial^2}{\partial x_p \partial x_q} \right] \mathbf{f}(\mathbf{x}) \Big|_{\mathbf{x}=\bar{\mathbf{x}}} \quad (21b)$$

or expressed with a Stirling interpolation:

$$\tilde{D}_{\Delta x} \mathbf{f} = \frac{1}{e^{i\theta} h} [\Delta x_p \mu_p \delta_p] \mathbf{f}(\bar{\mathbf{x}}) \quad (22a)$$

$$\tilde{D}_{\Delta x}^2 \mathbf{f} = \frac{1}{(e^{i\theta} h)^2} \left[ \sum_{p=1}^n (\Delta x_p)^2 \delta_p^2 + \sum_{p=1}^n \sum_{q=1, q \neq p}^n \Delta x_p \Delta x_q (\mu_p \delta_p)(\mu_q \delta_q) \right] \mathbf{f}(\bar{\mathbf{x}}) \quad (22b)$$

Restricting the series to second order gives

$$\mathbf{y} \approx \mathbf{f}(\bar{\mathbf{x}}) + \tilde{D}_{\Delta x} \mathbf{f}(\bar{\mathbf{x}}) + \frac{1}{2!} \tilde{D}_{\Delta x}^2 \mathbf{f}(\bar{\mathbf{x}}) \quad (23)$$

Equation (23) is just one of the many multi-variable extensions of the Taylor series.<sup>18</sup>

## IV. Approximation of Mean and Covariance

### IV.A. Truth Quantities

The estimated mean and error covariance will be compared to the “true” mean and error covariance for performance comparison. The true mean and error covariance are simply

$$\bar{\mathbf{x}} = \mathbb{E}\{\mathbf{x}\} \quad (24a)$$

$$P_{xx} = \mathbb{E}\{[\mathbf{x} - \bar{\mathbf{x}}][\mathbf{x} - \bar{\mathbf{x}}]^T\} \quad (24b)$$

where  $\mathbb{E}$  denotes expectation. Additionally, the true mean after the nonlinear transformation, and its error covariance and the cross covariance need to be determined:

$$\bar{\mathbf{y}}_T = \mathbb{E}\{\mathbf{f}(\mathbf{x})\} \quad (25a)$$

$$P_{yy,T} = \mathbb{E}\{[\mathbf{f}(\mathbf{x}) - \bar{\mathbf{y}}_T][\mathbf{f}(\mathbf{x}) - \bar{\mathbf{y}}_T]^T\} \quad (25b)$$

$$P_{xy,T} = \mathbb{E}\{[\mathbf{x} - \bar{\mathbf{x}}][\mathbf{f}(\mathbf{x}) - \bar{\mathbf{y}}_T]^T\} \quad (25c)$$

### IV.B. Statistical Decoupling

Equation (23) is one of the many multi-variable extensions using an interpolation approximation. Other extensions can be derived by using a linear transform of the original vector:

$$\mathbf{z} = S^{-1} \mathbf{x} \quad (26)$$

and the new nonlinear transformation,

$$\tilde{\mathbf{f}}(\mathbf{z}) \equiv \mathbf{f}(S\mathbf{z}) = \mathbf{f}(\mathbf{x}) \quad (27)$$

The Taylor series expansion for Eq. (27) is simply

$$\mathbf{y} \approx \tilde{\mathbf{f}}(\bar{\mathbf{z}}) + \tilde{D}_{\Delta z} \tilde{\mathbf{f}}(\bar{\mathbf{z}}) + \frac{1}{2!} \tilde{D}_{\Delta z}^2 \tilde{\mathbf{f}}(\bar{\mathbf{z}}) \quad (28)$$

Since Eq. (26) is just a linear constant transformation, the Taylor series expansions in Eqs. (23) and (28) are the same. However, this is not true with interpolation in place of the derivatives. For example, consider the first-order partial part of the Taylor series,

$$\begin{aligned} \tilde{D}_{\Delta x} \mathbf{f}(\bar{\mathbf{x}}) &= \frac{1}{e^{i\theta} h} \left[ \sum_{p=1}^n \Delta x_p \mu_p \delta_p \right] \mathbf{f}(\bar{\mathbf{x}}) \\ &= \frac{1}{2e^{i\theta} h} \sum_{p=1}^n \Delta x_p \left[ \mathbf{f}(\bar{\mathbf{x}} + e^{i\theta} h \boldsymbol{\varepsilon}_p) + \mathbf{f}(\bar{\mathbf{x}} - e^{i\theta} h \boldsymbol{\varepsilon}_p) \right] \end{aligned} \quad (29a)$$

$$\begin{aligned} \tilde{D}_{\Delta z} \tilde{\mathbf{f}}(\bar{\mathbf{z}}) &= \frac{1}{e^{i\theta} h} \left[ \sum_{p=1}^n \Delta z_p \mu_p \delta_p \right] \tilde{\mathbf{f}}(\bar{\mathbf{z}}) \\ &= \frac{1}{2e^{i\theta} h} \sum_{p=1}^n \Delta z_p \left[ \tilde{\mathbf{f}}(\bar{\mathbf{z}} + e^{i\theta} h \boldsymbol{\varepsilon}_p) + \tilde{\mathbf{f}}(\bar{\mathbf{z}} - e^{i\theta} h \boldsymbol{\varepsilon}_p) \right] \\ &= \frac{1}{2e^{i\theta} h} \sum_{p=1}^n \Delta z_p \left[ \mathbf{f}(S[\bar{\mathbf{z}} + e^{i\theta} h \boldsymbol{\varepsilon}_p]) + \mathbf{f}(S[\bar{\mathbf{z}} - e^{i\theta} h \boldsymbol{\varepsilon}_p]) \right] \\ &= \frac{1}{2e^{i\theta} h} \sum_{p=1}^n S^{-1} \Delta x_p \left[ \mathbf{f}(\bar{\mathbf{x}} + e^{i\theta} h \mathbf{s}_p) + \mathbf{f}(\bar{\mathbf{x}} - e^{i\theta} h \mathbf{s}_p) \right] \end{aligned} \quad (29b)$$

where  $\mathbf{s}_p$  is the  $p^{\text{th}}$  column of  $S$ . It is apparent from Eqs. (29) that Eq. (23) will be different than Eq. (28).

Any square symmetric positive-definite matrix can be decomposed into two triangular matrices, each equal to the transpose of the other,  $P = SS^T$ . This is called the Cholesky decomposition and the decomposed matrix is referred as the Cholesky factor,  $S$ . Many other decomposition schemes exist, but the Cholesky decomposition is proved to be a computationally more efficient. One particularly useful transformation of  $\mathbf{x}$  is by using the Cholesky factor of the state error-covariance matrix ( $P_{xx} = S_x S_x^T$ ) to *stochastically decouple*  $\mathbf{x}$  and  $\mathbf{z}$ ,

$$\mathbf{z} = S_x^{-1} \mathbf{x} \quad (30)$$

so that elements of  $\mathbf{z}$  are now mutually independent from each other and has unity variance with itself,

$$\mathbb{E} \{ [\mathbf{z} - \bar{\mathbf{z}}][\mathbf{z} - \bar{\mathbf{z}}]^T \} = I \quad , \quad \bar{\mathbf{z}} = \mathbb{E} \{ \mathbf{z} \} \quad (31)$$

or

$$\Delta \mathbf{z} \sim \mathcal{N}(\mathbf{0}, I) \quad (32)$$

with  $\Delta \mathbf{z} = \mathbf{z} - \bar{\mathbf{z}}$ ; notice that the symmetrically distributed  $\mathbf{z}$  translates their zero mean distribution. The advantage of this decoupling will be made clear in the subsequent analysis with  $\mathbf{z}$  instead of  $\mathbf{x}$  directly. Conversion back to  $\mathbf{x}$  upon completion of analysis is trivial. Also, during these analysis,  $\tilde{\mathbf{f}}(\bar{\mathbf{z}})$  is defined  $\forall \bar{\mathbf{z}} \in \mathbb{R}^n$ .

## V. Second-Order Approximation

The second-order polynomial approximation of the true nonlinear transformation is simply

$$\begin{aligned} \mathbf{y} &\approx \tilde{\mathbf{f}}(\bar{\mathbf{z}}) + \tilde{D}_{\Delta z} \tilde{\mathbf{f}} + \frac{1}{2} \tilde{D}_{\Delta z}^2 \tilde{\mathbf{f}} \\ &= \tilde{\mathbf{f}}(\bar{\mathbf{z}}) + \frac{1}{e^{i\theta} h} \left( \sum_{p=1}^n \Delta z_p \mu_p \delta_p \right) \tilde{\mathbf{f}}(\bar{\mathbf{z}}) \\ &\quad + \frac{1}{2(e^{i\theta} h)^2} \left( \sum_{p=1}^n (\Delta z_p)^2 \delta_p^2 + \sum_{p=1}^n \sum_{q=1, q \neq p}^n \Delta z_p \Delta z_q (\mu_p \delta_p)(\mu_q \delta_q) \right) \tilde{\mathbf{f}}(\bar{\mathbf{z}}) \end{aligned} \quad (33)$$

and its estimated quantity,  $\bar{\mathbf{y}} = E\{\mathbf{y}\}$ :

$$\begin{aligned}
\bar{\mathbf{y}} &= E\left\{\tilde{\mathbf{f}}(\bar{\mathbf{z}}) + \frac{1}{2(e^{i\theta}h)^2} \left(\sum_{p=1}^n (\Delta z_p)^2 \delta_p^2\right) \tilde{\mathbf{f}}(\bar{\mathbf{z}})\right\} \\
&= \tilde{\mathbf{f}}(\bar{\mathbf{z}}) + \frac{\sigma_2}{2(e^{i\theta}h)^2} \sum_{p=1}^n \delta_p^2 \tilde{\mathbf{f}}(\bar{\mathbf{z}}) \\
&= \tilde{\mathbf{f}}(\bar{\mathbf{z}}) + \frac{1}{2(e^{i\theta}h)^2} \sum_{p=1}^n \left[\tilde{\mathbf{f}}(\bar{\mathbf{z}} + e^{i\theta}h\mathbf{e}_p) + \tilde{\mathbf{f}}(\bar{\mathbf{z}} - e^{i\theta}h\mathbf{e}_p)\right] - \frac{n}{(e^{i\theta}h)^2} \tilde{\mathbf{f}}(\bar{\mathbf{z}}) \\
&= \frac{(e^{i\theta}h)^2 - n}{(e^{i\theta}h)^2} \tilde{\mathbf{f}}(\bar{\mathbf{z}}) + \frac{1}{2(e^{i\theta}h)^2} \sum_{p=1}^n \left[\tilde{\mathbf{f}}(\bar{\mathbf{z}} + e^{i\theta}h\mathbf{e}_p) + \tilde{\mathbf{f}}(\bar{\mathbf{z}} - e^{i\theta}h\mathbf{e}_p)\right] \\
&= \frac{(e^{i\theta}h)^2 - n}{(e^{i\theta}h)^2} \mathbf{f}(\bar{\mathbf{x}}) + \frac{1}{2(e^{i\theta}h)^2} \sum_{p=1}^n \left[\mathbf{f}(\bar{\mathbf{x}} + e^{i\theta}h\mathbf{s}_{x,p}) + \mathbf{f}(\bar{\mathbf{x}} - e^{i\theta}h\mathbf{s}_{x,p})\right] \tag{34}
\end{aligned}$$

From Eq. (33), notice that  $\tilde{\mathbf{f}}(\bar{\mathbf{z}})$  is a deterministic term, thus instead of  $\mathbf{y}$ ,  $\mathbf{y} - \tilde{\mathbf{f}}(\bar{\mathbf{z}})$  could be used in derivation of the covariance for  $\mathbf{y}$  as this would simplify the intermediate analysis:

$$\begin{aligned}
P_{yy,T} &= E\left\{[\mathbf{y} - E\{\mathbf{y}\}][\mathbf{y} - E\{\mathbf{y}\}]^T\right\} \\
&= E\{[\mathbf{y}][\mathbf{y}]^T\} - E\{\mathbf{y}\}E\{\mathbf{y}\}^T \\
&= E\left\{[\mathbf{y} - \tilde{\mathbf{f}}(\bar{\mathbf{z}})][\mathbf{y} - \tilde{\mathbf{f}}(\bar{\mathbf{z}})]^T\right\} - E\{\mathbf{y} - \tilde{\mathbf{f}}(\bar{\mathbf{z}})\}E\{\mathbf{y} - \tilde{\mathbf{f}}(\bar{\mathbf{z}})\}^T \tag{35}
\end{aligned}$$

This leaves the estimate covariance as

$$\begin{aligned}
P_{yy} &= E\left\{\left[\tilde{D}_{\Delta z}\tilde{\mathbf{f}} + \frac{1}{2}\tilde{D}_{\Delta z}^2\tilde{\mathbf{f}}\right]\left[\tilde{D}_{\Delta z}\tilde{\mathbf{f}} + \frac{1}{2}\tilde{D}_{\Delta z}^2\tilde{\mathbf{f}}\right]^T\right\} \\
&\quad - E\left\{\tilde{D}_{\Delta z}\tilde{\mathbf{f}} + \frac{1}{2}\tilde{D}_{\Delta z}^2\tilde{\mathbf{f}}\right\}E\left\{\tilde{D}_{\Delta z}\tilde{\mathbf{f}} + \frac{1}{2}\tilde{D}_{\Delta z}^2\tilde{\mathbf{f}}\right\}^T \\
&= E\left\{\overset{\textcircled{1}}{\left[\tilde{D}_{\Delta z}\tilde{\mathbf{f}}\right]\left[\tilde{D}_{\Delta z}\tilde{\mathbf{f}}\right]^T}\right\} + \frac{1}{4}E\left\{\overset{\textcircled{2}}{\left[\tilde{D}_{\Delta z}^2\tilde{\mathbf{f}}\right]\left[\tilde{D}_{\Delta z}^2\tilde{\mathbf{f}}\right]^T}\right\} - \frac{1}{4}E\left\{\overset{\textcircled{3}}{\tilde{D}_{\Delta z}^2\tilde{\mathbf{f}}}\right\}E\left\{\overset{\textcircled{3}}{\tilde{D}_{\Delta z}^2\tilde{\mathbf{f}}}\right\}^T \tag{36}
\end{aligned}$$

Note that all odd moments in Eq. (36) evaluate to zero due to the symmetric distribution of elements in  $\mathbf{z}$  and they are uncorrelated with each other. Given the length of the individual analysis, each of the term  $\textcircled{1}$ ,  $\textcircled{2}$  and  $\textcircled{3}$  will be evaluated separately. The  $p^{\text{th}}$  moment of an element of  $\mathbf{z}$  is denoted as  $\sigma_p$ . Also, as from Eq. (31), the second moment of each  $\mathbf{z}$  element is unity:

$$\begin{aligned}
\underline{\textcircled{1}} \quad E\left\{\left[\tilde{D}_{\Delta z}\tilde{\mathbf{f}}\right]\left[\tilde{D}_{\Delta z}\tilde{\mathbf{f}}\right]^T\right\} &= \frac{1}{(e^{i\theta}h)^2} E\left\{\left[\sum_{p=1}^n \Delta z_p \mu_p \delta_p \tilde{\mathbf{f}}(\bar{\mathbf{z}})\right]\left[\sum_{p=1}^n \Delta z_p \mu_p \delta_p \tilde{\mathbf{f}}(\bar{\mathbf{z}})\right]^T\right\} \\
&= \frac{\sigma_2}{(e^{i\theta}h)^2} \sum_{p=1}^n \left[\mu_p \delta_p \tilde{\mathbf{f}}(\bar{\mathbf{z}})\right]\left[\mu_p \delta_p \tilde{\mathbf{f}}(\bar{\mathbf{z}})\right]^T \\
&= \frac{1}{4(e^{i\theta}h)^2} \sum_{p=1}^n \left[\tilde{\mathbf{f}}(\bar{\mathbf{z}} + e^{i\theta}h\mathbf{e}_p)\right]\left[\tilde{\mathbf{f}}(\bar{\mathbf{z}} + e^{i\theta}h\mathbf{e}_p)\right]^T \\
&= \frac{1}{4(e^{i\theta}h)^2} \sum_{p=1}^n \left[\mathbf{f}(\bar{\mathbf{x}} + e^{i\theta}h\mathbf{s}_{x,p})\right]\left[\mathbf{f}(\bar{\mathbf{x}} + e^{i\theta}h\mathbf{s}_{x,p})\right]^T \tag{37}
\end{aligned}$$

where  $\mathbf{s}_{x,p}$  is the  $p^{\text{th}}$  column of the square Cholesky factor from Eq. (30).



②  $\underline{E \left\{ \left[ \tilde{D}_{\Delta z}^2 \tilde{\mathbf{f}} \right] \left[ \tilde{D}_{\Delta z}^2 \tilde{\mathbf{f}} \right]^T \right\}}$  consists of three kinds of terms,  $\forall p, \forall q, p \neq q$ ,

$$E \left\{ \left[ (\Delta z_p)^2 \delta_p^2 \tilde{\mathbf{f}} \right] \left[ (\Delta z_p)^2 \delta_p^2 \tilde{\mathbf{f}} \right]^T \right\} = \left[ \delta_p^2 \tilde{\mathbf{f}} \right] \left[ \delta_p^2 \tilde{\mathbf{f}} \right]^T \sigma_4 \quad (38a)$$

$$E \left\{ \left[ (\Delta z_p)^2 \delta_p^2 \tilde{\mathbf{f}} \right] \left[ (\Delta z_q)^2 \delta_q^2 \tilde{\mathbf{f}} \right]^T \right\} = \left[ \delta_p^2 \tilde{\mathbf{f}} \right] \left[ \delta_q^2 \tilde{\mathbf{f}} \right]^T \sigma_2^2 \quad (38b)$$

$$E \left\{ \left[ \Delta z_p \Delta z_q \mu_p \delta_q \mu_p \delta_q \tilde{\mathbf{f}} \right] \left[ \Delta z_p \Delta z_q \mu_p \delta_q \mu_p \delta_q \tilde{\mathbf{f}} \right]^T \right\} = \left[ \mu_p \delta_p \mu_q \delta_q \tilde{\mathbf{f}} \right] \left[ \mu_p \delta_p \mu_q \delta_q \tilde{\mathbf{f}} \right]^T \sigma_2^2 \quad (38c)$$

③  $\underline{E \left\{ \tilde{D}_{\Delta z}^2 \tilde{\mathbf{f}} \right\} E \left\{ \tilde{D}_{\Delta z}^2 \tilde{\mathbf{f}} \right\}^T}$  consists of two kinds of terms,  $\forall p, \forall q, p \neq q$ ,

$$E \left\{ (\Delta z_p)^2 \delta_p \tilde{\mathbf{f}} \right\} E \left\{ (\Delta z_p)^2 \delta_p \tilde{\mathbf{f}} \right\}^T = \left[ \delta_p^2 \tilde{\mathbf{f}} \right] \left[ \delta_p^2 \tilde{\mathbf{f}} \right]^T \sigma_2^2 \quad (39a)$$

$$E \left\{ (\Delta z_p)^2 \delta_p \tilde{\mathbf{f}} \right\} E \left\{ (\Delta z_q)^2 \delta_q \tilde{\mathbf{f}} \right\}^T = \left[ \delta_p^2 \tilde{\mathbf{f}} \right] \left[ \delta_q^2 \tilde{\mathbf{f}} \right]^T \sigma_2^2 \quad (39b)$$

Terms in Eqs. (38b) and (39b) cancel each other. Terms in Eq. (39b) will be discarded from analysis for the reason explained in Ref. 7. Basically they do not constitute to better filter accuracy, while they are computationally expensive to calculate. The Stirling operators portion from Eqs. (38a) and (39a) are expanded as

$$\begin{aligned} \left[ \delta_p^2 \tilde{\mathbf{f}}(\bar{\mathbf{z}}) \right] \left[ \delta_p^2 \tilde{\mathbf{f}}(\bar{\mathbf{z}}) \right]^T &= \left[ \tilde{\mathbf{f}}(\bar{\mathbf{z}} + e^{i\theta} h \boldsymbol{\varepsilon}_p) - \tilde{\mathbf{f}}(\bar{\mathbf{z}} - e^{i\theta} h \boldsymbol{\varepsilon}_p) \right] \left[ \tilde{\mathbf{f}}(\bar{\mathbf{z}} + e^{i\theta} h \boldsymbol{\varepsilon}_p) - \tilde{\mathbf{f}}(\bar{\mathbf{z}} - e^{i\theta} h \boldsymbol{\varepsilon}_p) \right]^T \\ &= \left[ \mathbf{f}(\bar{\mathbf{x}} + e^{i\theta} h \mathbf{s}_{x,p}) - \mathbf{f}(\bar{\mathbf{x}} - e^{i\theta} h \mathbf{s}_{x,p}) \right] \left[ \mathbf{f}(\bar{\mathbf{x}} + e^{i\theta} h \mathbf{s}_{x,p}) - \mathbf{f}(\bar{\mathbf{x}} - e^{i\theta} h \mathbf{s}_{x,p}) \right]^T \end{aligned} \quad (40)$$

Again,  $\sigma_2 = 1$  from the way  $\mathbf{z}$  is generated. If the distribution is Gaussian, then  $\sigma_4 = h^2$  and  $h^2 = 3$ ; for the analysis refer to §3.3 of Ref. 7. Finally  $P_{yy}$  becomes

$$\begin{aligned} P_{yy} &= \frac{1}{4(e^{i\theta} h)^2} \sum_{p=1}^n \left[ \mathbf{f}(\bar{\mathbf{x}} + e^{i\theta} h \mathbf{s}_{x,p}) - \mathbf{f}(\bar{\mathbf{x}} - e^{i\theta} h \mathbf{s}_{x,p}) \right] \left[ \mathbf{f}(\bar{\mathbf{x}} + e^{i\theta} h \mathbf{s}_{x,p}) - \mathbf{f}(\bar{\mathbf{x}} - e^{i\theta} h \mathbf{s}_{x,p}) \right]^T \\ &\quad + \frac{(e^{i\theta} h)^2 - 1}{2(e^{i\theta} h)^4} \sum_{p=1}^n \left[ \mathbf{f}(\bar{\mathbf{x}} + e^{i\theta} h \mathbf{s}_{x,p}) + \mathbf{f}(\bar{\mathbf{x}} - e^{i\theta} h \mathbf{s}_{x,p}) - 2\mathbf{f}(\bar{\mathbf{x}}) \right] \left[ \mathbf{f}(\bar{\mathbf{x}} + e^{i\theta} h \mathbf{s}_{x,p}) + \mathbf{f}(\bar{\mathbf{x}} - e^{i\theta} h \mathbf{s}_{x,p}) - 2\mathbf{f}(\bar{\mathbf{x}}) \right]^T \end{aligned} \quad (41)$$

Similarly, the cross-covariance can be derived as

$$\begin{aligned} P_{xy} &= E \left\{ [\mathbf{x} - \bar{\mathbf{x}}][\mathbf{y} - \bar{\mathbf{y}}]^T \right\} \\ &= E \left\{ [S_x \Delta \mathbf{z}] \left[ \tilde{\mathbf{f}}(\bar{\mathbf{z}}) + \tilde{D}_{\Delta z} \mathbf{f} + \frac{1}{2} \tilde{D}_{\Delta z}^2 \mathbf{f} - \tilde{\mathbf{f}}(\bar{\mathbf{z}}) - \frac{1}{2} E \left\{ \tilde{D}_{\Delta z}^2 \mathbf{f} \right\} \right]^T \right\} \\ &= E \left\{ [S_x \Delta \mathbf{z}] \left[ \tilde{D}_{\Delta z} \tilde{\mathbf{f}} \right]^T \right\} \\ &= \frac{1}{2e^{i\theta} h} \sum_{p=1}^n [\mathbf{s}_{x,p}] \left[ \mathbf{f}(\bar{\mathbf{x}} + e^{i\theta} h \mathbf{s}_{x,p}) - \mathbf{f}(\bar{\mathbf{x}} - e^{i\theta} h \mathbf{s}_{x,p}) \right]^T \end{aligned} \quad (42)$$

again, odd moments evaluated to zero.

## VI. Second-Order Complex Divided-Difference Filter

This section summarizes the algorithm for a second-order complex-step filter based on the DD2 filter. For the resemblance with the DD2 filter, the interested reader is again referred to Ref. 7 for complete derivations. The filter starts off with initializations of states, process noise covariance, measurement covariance and states

error covariance. The filter then enters into the measurement update and propagation loop until the last available measurement. The measurement update is sometimes referred as the *a posteriori* update while propagation is also called the *a priori* update or time update. Common notations are superscript “+” which denotes updated values, “-” which denotes propagated values and “*k*” which denotes time index. A computationally efficient Cholesky square factor is used to maintain (and update if necessary) the covariances at the square-root level. A Householder triangulation is used as an efficient way to maintain the square Cholesky factor for the rectangular matrix.

### VI.1. Dynamical and Measurement Models

1. The system dynamics and measurement model are modeled as

$$\mathbf{x}(k+1) = \mathbf{f}[\mathbf{x}(k), \mathbf{u}(k), \mathbf{v}(k)], \quad \mathbf{v}(k) \sim \mathcal{N}[\bar{\mathbf{v}}(k), Q(k)] \quad (43)$$

$$\tilde{\mathbf{y}}(k) = \mathbf{g}[\mathbf{x}(k), \mathbf{w}(k)], \quad \mathbf{w}(k) \sim \mathcal{N}[\bar{\mathbf{w}}(k), R(k)] \quad (44)$$

where  $\mathbf{v}(k)$  and  $\mathbf{w}(k)$  are i.i.d. (independent & identically distributed) random noise with given means and covariances, and  $\mathbf{u}(k)$  is a known input vector.

### VI.2. Initialization

1. Initialize the states, error covariance

$$\hat{\mathbf{x}}^-(0) = \hat{\mathbf{x}}_0^-, \quad P^-(0) = P_0^- \quad (45)$$

2. Cholesky decomposition of the process noise covariance, measurement noise covariance and error covariance:

$$Q(k) = S_v(k)S_v^T(k), \quad R(k) = S_w(k)S_w^T(k) \quad (46)$$

$$P^-(k) = S_x^-(k)S_x^{-T}(k), \quad P^+(k) = S_x^+(k)S_x^{+T}(k) \quad (47)$$

### VI.3. Measurement Update

1. Given  $\hat{\mathbf{x}}^-(k)$ ,  $S_x^-(k)$ ,  $\bar{\mathbf{w}}(k)$ ,  $\theta$  and  $h$ , compute the following quantities:

$$\mathbf{s}_{yx,p}^{(1)-}(k) \equiv \frac{1}{2e^{i\theta}h} \{ \mathbf{g}[\hat{\mathbf{x}}^-(k) + e^{i\theta}h \mathbf{s}_{x,q}^-(k), \bar{\mathbf{w}}(k)] - \mathbf{g}[\hat{\mathbf{x}}^-(k) - e^{i\theta}h \mathbf{s}_{x,q}^-(k), \bar{\mathbf{w}}(k)] \} \quad (48a)$$

$$\mathbf{s}_{yx,p}^{(2)-}(k) \equiv \frac{\sqrt{(e^{i\theta}h)^2 - 1}}{2(e^{i\theta}h)^2} \{ \mathbf{g}[\hat{\mathbf{x}}^-(k) + e^{i\theta}h \mathbf{s}_{x,q}^-(k), \bar{\mathbf{w}}(k)] + \mathbf{g}[\hat{\mathbf{x}}^-(k) - e^{i\theta}h \mathbf{s}_{x,q}^-(k), \bar{\mathbf{w}}(k)] - 2\mathbf{g}[\hat{\mathbf{x}}^-(k), \bar{\mathbf{w}}(k)] \} \quad (48b)$$

$$S_{yx}^{(1)-}(k) = \begin{bmatrix} \mathbf{s}_{yx,1}^{(1)-}(k) & \mathbf{s}_{yx,2}^{(1)-}(k) & \cdots & \mathbf{s}_{yx,n_x}^{(1)-}(k) \end{bmatrix}, \quad S_{yx}^{(2)-}(k) = \begin{bmatrix} \mathbf{s}_{yx,1}^{(2)-}(k) & \mathbf{s}_{yx,2}^{(2)-}(k) & \cdots & \mathbf{s}_{yx,n_x}^{(2)-}(k) \end{bmatrix} \quad (48c)$$

$$\mathbf{s}_{yw,p}^{(1)-}(k) \equiv \frac{1}{2e^{i\theta}h} \{ \mathbf{g}[\hat{\mathbf{x}}^-(k), \bar{\mathbf{w}}(k) + e^{i\theta}h \mathbf{s}_{w,q}(k)] - \mathbf{g}[\hat{\mathbf{x}}^-(k), \bar{\mathbf{w}}(k) - e^{i\theta}h \mathbf{s}_{w,q}(k)] \} \quad (48d)$$

$$\mathbf{s}_{yw,p}^{(2)-}(k) \equiv \frac{\sqrt{(e^{i\theta}h)^2 - 1}}{2(e^{i\theta}h)^2} \{ \mathbf{g}[\hat{\mathbf{x}}^-(k), \bar{\mathbf{w}}(k) + e^{i\theta}h \mathbf{s}_{w,q}(k)] + \mathbf{g}[\hat{\mathbf{x}}^-(k), \bar{\mathbf{w}}(k) - e^{i\theta}h \mathbf{s}_{w,q}(k)] - 2\mathbf{g}[\hat{\mathbf{x}}^-(k), \bar{\mathbf{w}}(k)] \} \quad (48e)$$

$$S_{yw}^{(1)-}(k) = \begin{bmatrix} \mathbf{s}_{yw,1}^{(1)-}(k) & \mathbf{s}_{yw,2}^{(1)-}(k) & \cdots & \mathbf{s}_{yw,n_w}^{(1)-}(k) \end{bmatrix}, \quad S_{yw}^{(2)-}(k) = \begin{bmatrix} \mathbf{s}_{yw,1}^{(2)-}(k) & \mathbf{s}_{yw,2}^{(2)-}(k) & \cdots & \mathbf{s}_{yw,n_w}^{(2)-}(k) \end{bmatrix} \quad (48f)$$

where  $n_x$  and  $n_w$  are the dimension of the state and measurement noise, respectively,  $\mathbf{s}_{x,q}^-(k)$  denotes the  $q^{\text{th}}$  column of  $S_x^-(k)$ ,  $\mathbf{s}_{yx,p}^{(1)-}(k)$  and  $\mathbf{s}_{yx,p}^{(2)-}(k)$  denote the  $p^{\text{th}}$  column of  $S_{yx}^{(1)-}(k)$  and  $S_{yx}^{(2)-}(k)$ , respectively,  $\mathbf{s}_{w,q}(k)$  denotes the  $q^{\text{th}}$  column of  $S_w(k)$ , and  $\mathbf{s}_{yw,p}^{(1)-}(k)$  and  $\mathbf{s}_{yw,p}^{(2)-}(k)$  denote the  $p^{\text{th}}$  column of  $S_{yw}^{(1)-}(k)$  and  $S_{yw}^{(2)-}(k)$ , respectively.

2. Compute the output estimate

$$\begin{aligned}\hat{\mathbf{y}}^-(k) &= \frac{(e^{i\theta}h)^2 - n_x - n_w}{(e^{i\theta}h)^2} \mathbf{g}[\hat{\mathbf{x}}^-(k), \bar{\mathbf{w}}(k)] \\ &+ \frac{1}{2(e^{i\theta}h)^2} \sum_{p=1}^{n_x} \mathbf{g}[\hat{\mathbf{x}}^-(k) + e^{i\theta}h \mathbf{s}_{x,p}^-(k), \bar{\mathbf{w}}(k)] + \mathbf{g}[\hat{\mathbf{x}}^-(k) - e^{i\theta}h \mathbf{s}_{x,p}^-(k), \bar{\mathbf{w}}(k)] \\ &+ \frac{1}{2(e^{i\theta}h)^2} \sum_{p=1}^{n_w} \mathbf{g}[\hat{\mathbf{x}}^-(k), \bar{\mathbf{w}}(k) + e^{i\theta}h \mathbf{s}_{w,p}(k)] + \mathbf{g}[\hat{\mathbf{x}}^-(k), \bar{\mathbf{w}}(k) - e^{i\theta}h \mathbf{s}_{w,p}(k)]\end{aligned}\quad (49)$$

3. Perform a Householder Triangulation

$$S_y(k) = \mathcal{H} \left\{ \begin{bmatrix} S_{yx}^{(1)-}(k) & S_{yw}^{(1)-}(k) & S_{yx}^{(2)-}(k) & S_{yw}^{(2)-}(k) \end{bmatrix} \right\} \quad (50)$$

where  $\mathcal{H}\{\cdot\}$  denotes the Householder Triangulation operation.

4. Calculate the Kalman gain

$$P_{xy}(k) = S_x^-(k) S_{yx}^{-T}(k) \quad (51)$$

$$K(k) = P_{xy}(k) [S_y(k) S_y^T(k)]^{-1} \quad (52)$$

where  $S_{yx}^{-T}(k) = \begin{bmatrix} S_{yx}^{(1)-}(k) & S_{yx}^{(2)-}(k) \end{bmatrix}^T$ .

5. Calculate the updates

$$\hat{\mathbf{x}}^+(k) = \hat{\mathbf{x}}^-(k) + K(k)[\tilde{\mathbf{y}}(k) - \hat{\mathbf{y}}^-(k)] \quad (53)$$

$$S_x^+(k) = \mathcal{H} \left\{ \begin{bmatrix} S_x^-(k) - K(k) S_{yx}^{(1)-}(k) & K(k) S_{yw}^{(1)-}(k) & K(k) S_{yx}^{(2)-}(k) & K(k) S_{yw}^{(2)-}(k) \end{bmatrix} \right\} \quad (54)$$

6. If the error covariance matrix is desired, it can be computed via  $P^+ = S_x^+ S_x^{+T}$  or

$$\begin{aligned}P^+(k) &= \begin{bmatrix} S_x^-(k) - K(k) S_{yx}^{(1)-}(k) \\ K(k) S_{yx}^{(2)-}(k) \end{bmatrix} \begin{bmatrix} S_x^-(k) - K(k) S_{yx}^{(1)-}(k) \\ K(k) S_{yx}^{(2)-}(k) \end{bmatrix}^T + \begin{bmatrix} K(k) S_{yw}^{(1)-}(k) \\ K(k) S_{yw}^{(2)-}(k) \end{bmatrix} \begin{bmatrix} K(k) S_{yw}^{(1)-}(k) \\ K(k) S_{yw}^{(2)-}(k) \end{bmatrix}^T \\ &+ \begin{bmatrix} K(k) S_{yx}^{(1)-}(k) \\ K(k) S_{yx}^{(2)-}(k) \end{bmatrix} \begin{bmatrix} K(k) S_{yx}^{(1)-}(k) \\ K(k) S_{yx}^{(2)-}(k) \end{bmatrix}^T + \begin{bmatrix} K(k) S_{yw}^{(1)-}(k) \\ K(k) S_{yw}^{(2)-}(k) \end{bmatrix} \begin{bmatrix} K(k) S_{yw}^{(1)-}(k) \\ K(k) S_{yw}^{(2)-}(k) \end{bmatrix}^T\end{aligned}\quad (55)$$

#### VI..4. Propagation

1. Calculate the following quantities

$$\mathbf{s}_{xx,p}^{(1)+}(k) \equiv \frac{1}{2e^{i\theta}h} \{ \mathbf{f}[\hat{\mathbf{x}}^+(k) + e^{i\theta}h \mathbf{s}_{x,q}^+(k), \mathbf{u}(k), \bar{\mathbf{v}}(k)] - \mathbf{f}[\hat{\mathbf{x}}^+(k) - e^{i\theta}h \mathbf{s}_{x,q}^+(k), \mathbf{u}(k), \bar{\mathbf{v}}(k)] \} \quad (56a)$$

$$\begin{aligned}\mathbf{s}_{xx,p}^{(2)+}(k) &\equiv \frac{\sqrt{(e^{i\theta}h)^2 - n_x - n_w}}{2(e^{i\theta}h)^2} \{ \mathbf{f}[\hat{\mathbf{x}}^+(k) + e^{i\theta}h \mathbf{s}_{x,q}^+(k), \mathbf{u}(k), \bar{\mathbf{v}}(k)] + \mathbf{f}[\hat{\mathbf{x}}^+(k) - e^{i\theta}h \mathbf{s}_{x,q}^+(k), \mathbf{u}(k), \bar{\mathbf{v}}(k)] \\ &- 2\mathbf{f}[\hat{\mathbf{x}}^+(k), \mathbf{u}(k), \bar{\mathbf{v}}(k)] \}\end{aligned}\quad (56b)$$

$$S_{xx}^{(1)+}(k) = \begin{bmatrix} \mathbf{s}_{xx,1}^{(1)+}(k) & \mathbf{s}_{xx,2}^{(1)+}(k) & \cdots & \mathbf{s}_{xx,n_x}^{(1)+}(k) \end{bmatrix}, \quad S_{xx}^{(2)+}(k) = \begin{bmatrix} \mathbf{s}_{xx,1}^{(2)+}(k) & \mathbf{s}_{xx,2}^{(2)+}(k) & \cdots & \mathbf{s}_{xx,n_x}^{(2)+}(k) \end{bmatrix} \quad (56c)$$

$$\mathbf{s}_{xv,p}^{(1)+}(k) \equiv \frac{1}{2e^{i\theta}h} \{ \mathbf{f}[\hat{\mathbf{x}}^+(k), \mathbf{u}(k), \bar{\mathbf{v}}(k) + e^{i\theta}h \mathbf{s}_{v,q}(k)] - \mathbf{f}[\hat{\mathbf{x}}^+(k), \mathbf{u}(k), \bar{\mathbf{v}}(k) - e^{i\theta}h \mathbf{s}_{v,q}(k)] \} \quad (56d)$$

$$\begin{aligned}\mathbf{s}_{xv,p}^{(2)+}(k) &\equiv \frac{\sqrt{(e^{i\theta}h)^2 - n_x - n_w}}{2(e^{i\theta}h)^2} \{ \mathbf{f}[\hat{\mathbf{x}}^+(k), \mathbf{u}(k), \bar{\mathbf{v}}(k) + e^{i\theta}h \mathbf{s}_{v,q}(k)] + \mathbf{f}[\hat{\mathbf{x}}^+(k), \mathbf{u}(k), \bar{\mathbf{v}}(k) - e^{i\theta}h \mathbf{s}_{v,q}(k)] \\ &- 2\mathbf{f}[\hat{\mathbf{x}}^+(k), \mathbf{u}(k), \bar{\mathbf{v}}(k)] \}\end{aligned}\quad (56e)$$

$$S_{xv}^{(1)+}(k) = \begin{bmatrix} \mathbf{s}_{xv,1}^{(1)+}(k) & \mathbf{s}_{xv,2}^{(1)+}(k) & \cdots & \mathbf{s}_{xv,n_v}^{(1)+}(k) \end{bmatrix}, \quad S_{xv}^{(2)+}(k) = \begin{bmatrix} \mathbf{s}_{xv,1}^{(2)+}(k) & \mathbf{s}_{xv,2}^{(2)+}(k) & \cdots & \mathbf{s}_{xv,n_v}^{(2)+}(k) \end{bmatrix} \quad (56f)$$

where  $n_v$  is the dimension of the process noise,  $\mathbf{s}_{x,q}^+(k)$  denotes the  $q^{\text{th}}$  column of  $S_x^+(k)$ ,  $\mathbf{s}_{xx,p}^{(1)+}(k)$  and  $\mathbf{s}_{xx,p}^{(2)+}(k)$  denote the  $p^{\text{th}}$  column of  $S_{xx}^{(1)+}(k)$  and  $S_{xx}^{(2)+}(k)$ , respectively,  $\mathbf{s}_{v,q}(k)$  denotes the  $q^{\text{th}}$  column of  $S_v(k)$ , and  $\mathbf{s}_{xv,p}^{(1)+}(k)$  and  $\mathbf{s}_{xv,p}^{(2)+}(k)$  denote the  $p^{\text{th}}$  column of  $S_{xv}^{(1)+}(k)$  and  $S_{xv}^{(2)+}(k)$ , respectively.

2. Propagate the states

$$\begin{aligned} \hat{\mathbf{x}}_{k+1}^- &= \frac{(e^{i\theta}h)^2 - n_x - n_v}{(e^{i\theta}h)^2} \mathbf{f}[\hat{\mathbf{x}}^+(k), \mathbf{u}(k), \bar{\mathbf{v}}(k)] \\ &+ \frac{1}{2(e^{i\theta}h)^2} \sum_{p=1}^{n_x} \mathbf{f}[\mathbf{x}^+(k) + e^{i\theta}h \mathbf{s}_{x,p}^+(k), \mathbf{u}(k), \bar{\mathbf{v}}(k)] + \mathbf{f}[\hat{\mathbf{x}}^+(k) - e^{i\theta}h \mathbf{s}_{x,p}^+(k), \mathbf{u}(k), \bar{\mathbf{v}}(k)] \\ &+ \frac{1}{2(e^{i\theta}h)^2} \sum_{p=1}^{n_v} \mathbf{f}[\hat{\mathbf{x}}^+(k), \mathbf{u}(k), \bar{\mathbf{v}}(k) + e^{i\theta}h \mathbf{s}_{v,p}(k)] + \mathbf{f}[\hat{\mathbf{x}}^+(k), \mathbf{u}(k), \bar{\mathbf{v}}(k) - e^{i\theta}h \mathbf{s}_{v,p}(k)] \end{aligned} \quad (57)$$

3. The propagation of  $S_x$  follows

$$S_x^-(k+1) = \mathcal{H} \left\{ \begin{bmatrix} S_{xx}^{(1)+}(k) & S_{xv}^{(1)+}(k) & S_{xx}^{(2)+}(k) & S_{xv}^{(2)+}(k) \end{bmatrix} \right\} \quad (58)$$

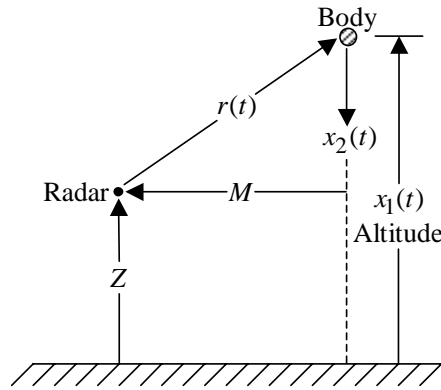


Figure 3. Vertically Falling Body Example

## VII. Performance Evaluation

This section presents some performance related figures to compare the performance of the standard DD2 and CSDA filters. The sample problem chosen for the comparison is Athan's problem,<sup>20</sup> which involves estimation of altitude, velocity and the ballistic coefficient of a vertically falling body, as shown in Figure 3. The equations of motion of the system are given by

$$\dot{x}_1(t) = -x_2(t) \quad (59a)$$

$$\dot{x}_2(t) = -e^{-\alpha x_1(t)} x_2^2(t) x_3(t) \quad (59b)$$

$$\dot{x}_3(t) = 0 \quad (59c)$$

where  $x_1(t)$  is the altitude,  $x_2(t)$  is the downward velocity,  $x_3(t)$  is the constant ballistic coefficient and  $\alpha = 5 \times 10^{-5}$  is a constant that relates air density with altitude. The range observation model is given by

$$\tilde{y}_k = \sqrt{M^2 + (x_{1,k} - Z)^2} + \nu_k \quad (60)$$

where  $\nu_k$  is the observation noise, and  $M$  and  $Z$  are constants. These parameters are given by  $M = 1 \times 10^5$  and  $Z = 1 \times 10^5$ . The variance of  $\nu_k$  is given by  $1 \times 10^4$ .

All simulations are run with a sampling interval of 1 sec with a total run time of 50 sec. Fifty Monte Carlo runs are performed and their average is used for performance comparison. A 4<sup>th</sup>-order Runge-Kutta

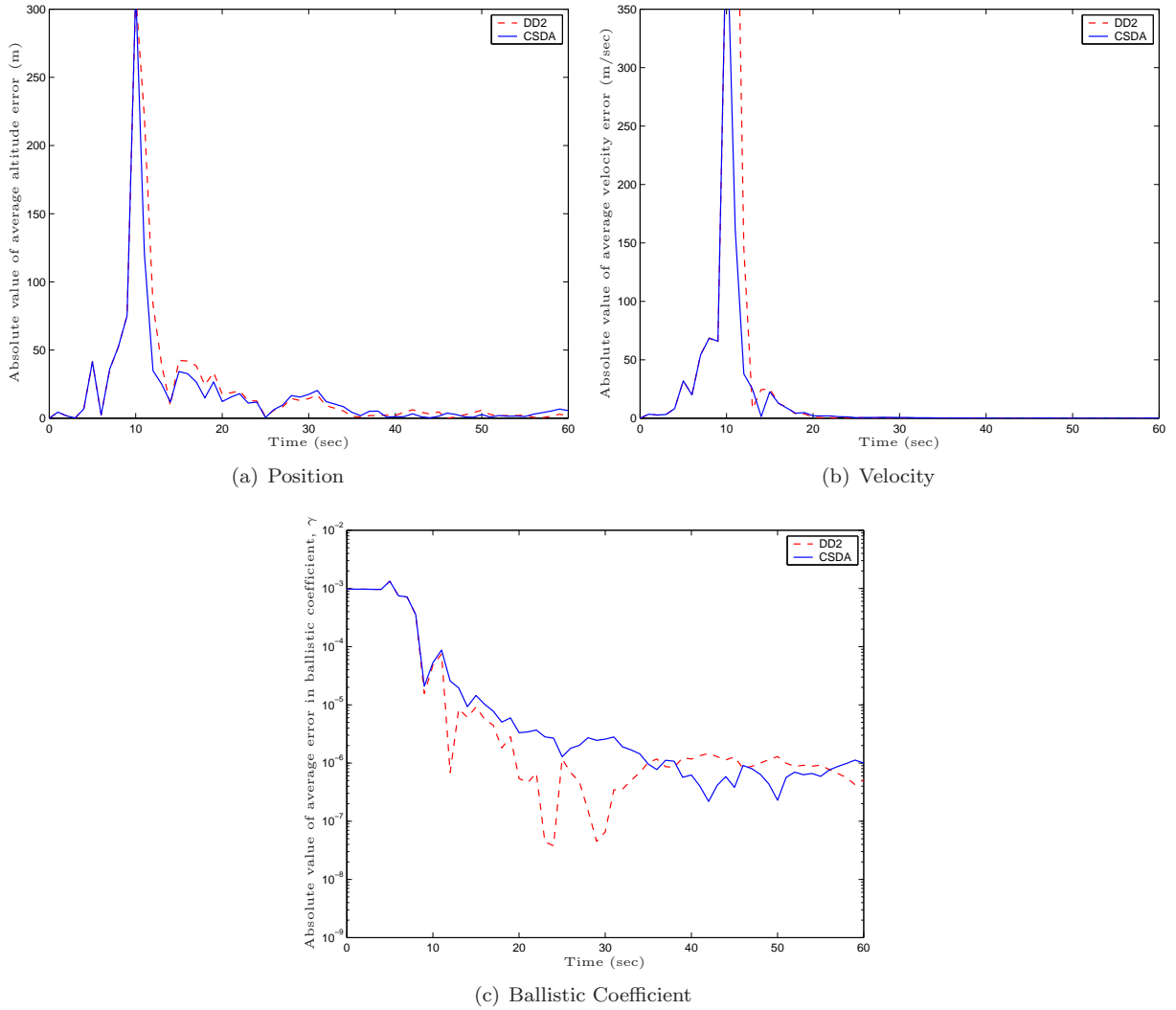


Figure 4. Sample state estimates from DD2 and CSDA filters. Simulations performed with  $h^2 = 2$ , CSDA angle =  $45^\circ$  and measurement variance  $R = 1 \times 10^4$

integration routine is used to propagate the states between each sampling interval. A few variables that are manipulated to assess the performance comparison include  $h^2$ , the CSDA angle  $\theta$  and the measurement covariance. Nominally,  $h^2 = \sqrt{3}$  for a Gaussian distribution and the measurement covariance is  $1 \times 10^4 \text{ m}^2$ , except when its influence on performance is being evaluated.

Figure 4 shows a sample of state estimation from both the DD2 and CSDA filters. The CSDA angle is set to  $90^\circ$ . The simulation is run with measurement model covariance of  $2 \times 10^4 \text{ m}^2$  instead of the “nominal” value of  $1 \times 10^4 \text{ m}^2$ . Figures 5-9 show the performance comparison between DD2 and CSDA filter. Figure 5 compares the total absolute between the two filters but subsequent figures compare them in terms of percentage. For Figs. 5 and 6, the CSDA angle of  $45^\circ$  is used since it has same magnitude for both the real and imaginary components. In these figures,  $h^2$  is increased from 1 until one of the filter becomes unstable. This is also a way to evaluate the Gaussianity of the system. Then in Fig. 7, the CSDA angle is varied from  $0^\circ$  (which is essentially standard DD2 filter) to  $180^\circ$  to look for the most suitable angle. Next in Fig. 8, different  $h^2$  values are tested again. Finally in Fig. 9, the measurement covariance is slowly increased from  $1 \times 10^4 \text{ m}^2$  to the point of an unstable filter condition. The absolute error is first used as a performance measure to gauge range of performance. This is the total error over the 50 sec filter run averaging from 50 Monte Carlo simulations. Later, only the percentage difference is used to more accurately present the relative performance change. The DD2 results are first used as a performance base for each of the comparisons.

Figure 4 gives the first glance into behavior of the DD2 and CSDA filters. It clearly shows that the

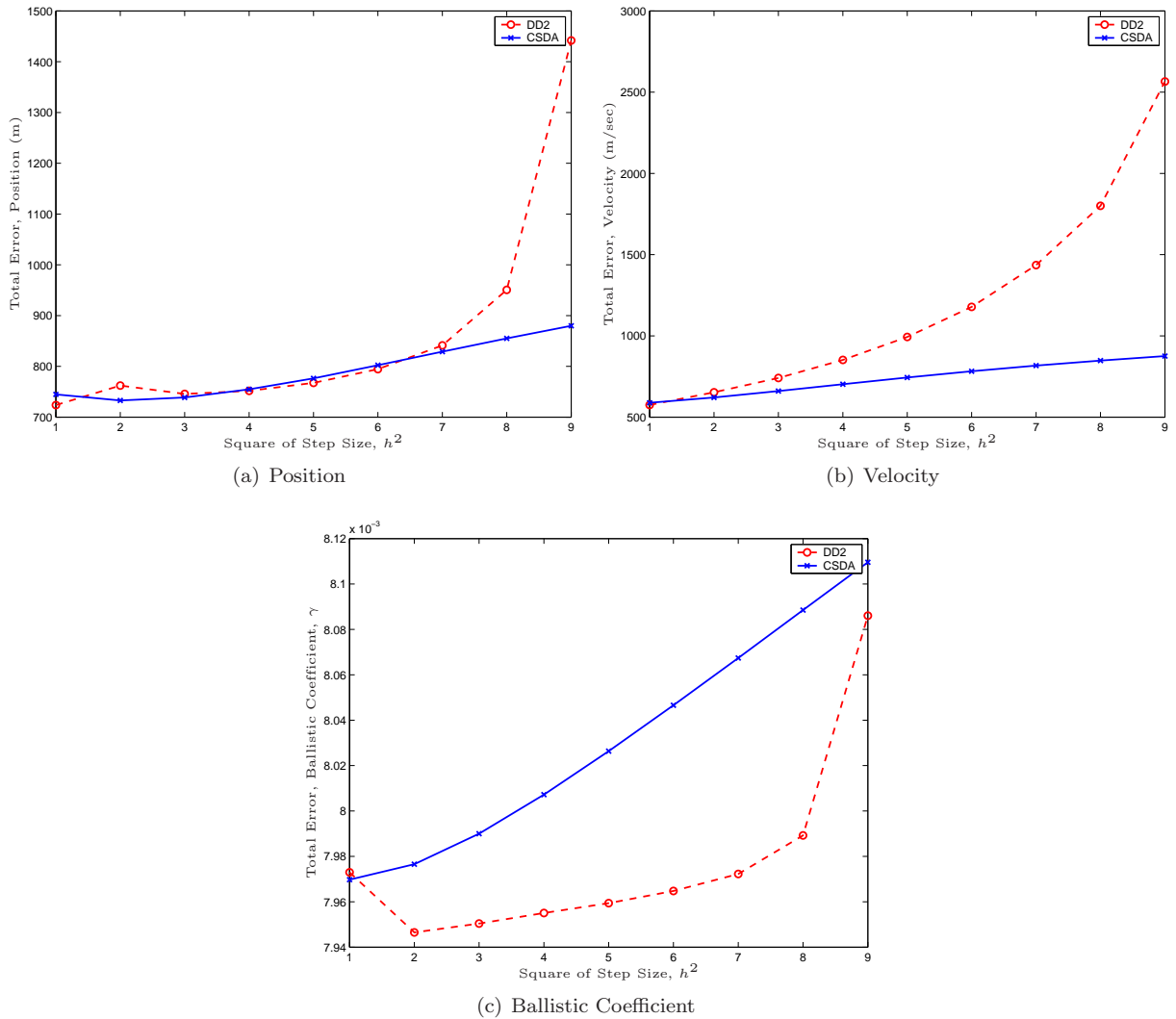
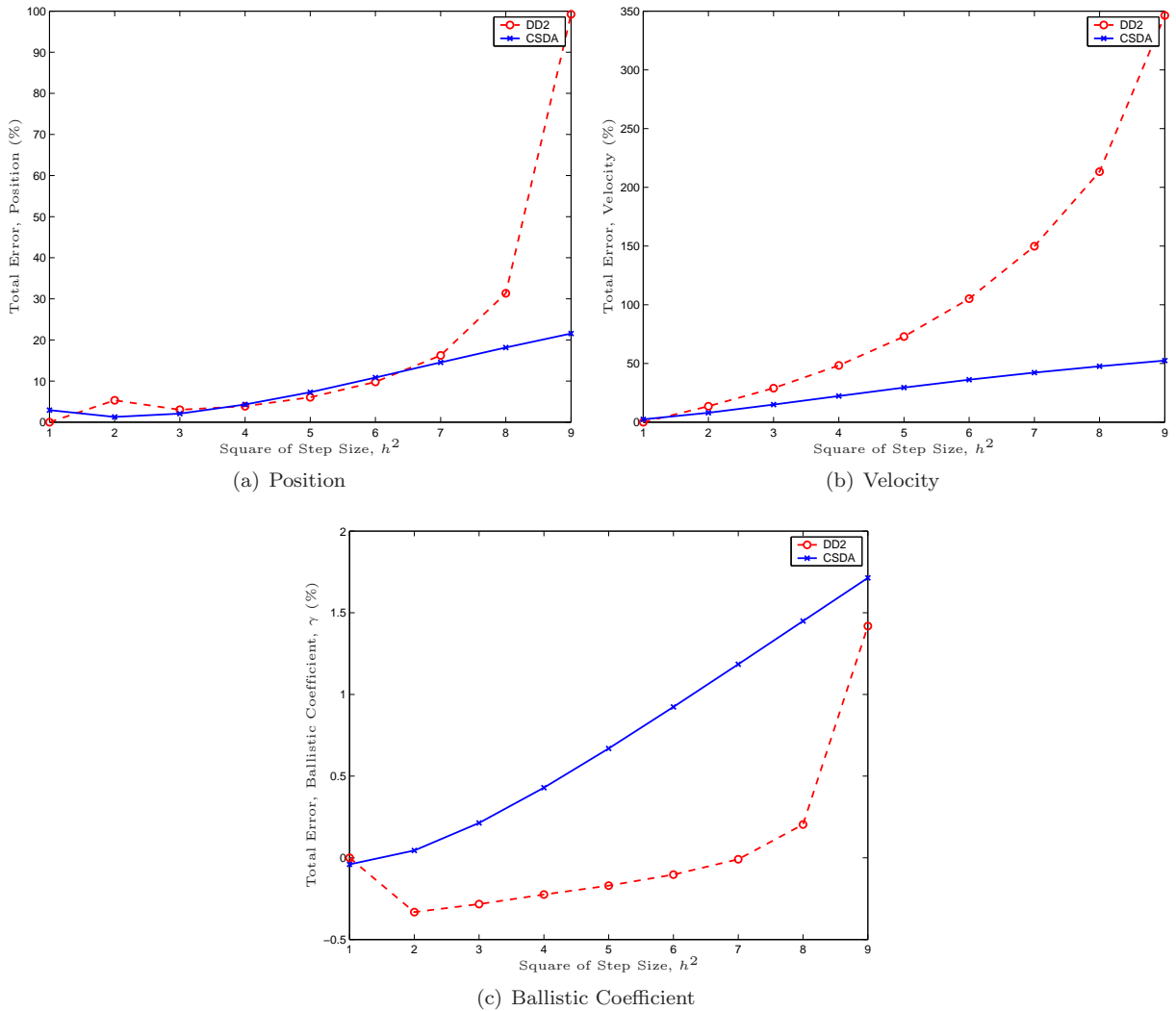


Figure 5. Absolute error, varying  $h^2$ . Simulations performed with CSDA angle =  $45^\circ$  and measurement variance  $R = 1 \times 10^4$ .

CSDA filter is better in both position and velocity estimates. At about 10 seconds into simulation the system experiences the lowest observability and thus is most challenging for the filters. Physically, this occurs when the object is on the same horizontal level as the radar. The CSDA filter consistently outperforms the DD2 filter during this low observability period. This indicates that the CSDA is able to better capture the system nonlinearity. However, Fig. 4(c) does not show a clear advantage for estimation of the ballistic coefficient. The total absolute error in the ballistic coefficient estimation in almost every case favors the DD2 filter. Though it is merely by a small percentage margin as shown in subsequent runs. The DD2 filter shows more abrupt movement in estimating the ballistic coefficient, which is more smooth for the CSDA filter.

Figure 5 evaluates the effect of  $h^2$  in the form of total estimation error of each state. Figure 6 shows the same information but as a percentage change based on the first DD2 results. From now onwards, the percentage change will be used as relative performance index. A value of  $h^2 = \sqrt{3}$  is optimal for Gaussian systems, but obviously our nonlinear system is not be very Gaussian. In reference to Fig. 6, low  $h^2$  values work better for both filters. At  $h^2 = 1$ , both filters exhibit the best possible performance characteristics for position and velocity estimation. Conversely, estimation error of ballistic coefficient is minimized at  $h^2 = 2$ . Estimation error in the ballistic coefficient for CSDA filter, however, bottoms at  $h^2 = 1$  and increases with increasing  $h^2$ . For these reasons,  $h^2 = 2$  embodies a good compromise for all three states and this will be used for succeeding runs. The DD2 filter becomes unstable at  $h^2$  beyond 9, but the CSDA filter is still able to give reasonable estimates. Moreover, the performance deteriorates much slower than the DD2 filter, once



**Figure 6.** Percentage of error, varying  $h^2$ . Simulations performed with CSDA angle =  $45^\circ$  and measurement variance  $R = 1 \times 10^4$ .

again showing the robustness of the CSDA filter.

The optimal angle for the CSDA filter is now examined. Figure 7 shows the effect of different angles from  $0^\circ$  (this reduces down to just plain DD2 filter) to  $180^\circ$ . It clearly reveals that  $90^\circ$  is the most optimal angle, which means using just a purely imaginary number,  $i$ . At this angle, the position estimate is improved by over 5% while the velocity estimate is improved impressively by over 12%. The less than 0.7% deterioration of the ballistic coefficient estimate is negligible compared to the vast performance gained in both position and velocity estimate. Thus  $e^{90^\circ}ih$  or just  $ih$  should be used as the step size. It is important to note that this angle is “optimal” only for this particular estimation problem. Other problems may require different values for this angle.

The effect of  $h^2$  with the optimal CSDA angle is now shown. Figure 8 shows that the sensitivity of the newly improved CSDA filter to various  $h^2$  is significantly reduced. The CSDA has so far shown to be more robust than DD2 filter in almost every measure. The last test is the influence of measurement noise. The measurement noise is slowly increased until the filters become unstable. From Fig. 9, the DD2 filter becomes unstable with measurement variance,  $R$ , greater than  $3 \times 10^4$ , however, it takes  $R$  to be greater than  $6 \times 10^4$  to make the CSDA filter unstable. Figures 9(a) and 9(b) show the “terminal” position and velocity estimates of the CSDA filter are still within the limit of operation for the DD2 filter, however, the ballistic coefficient estimate for the CSDA filter at  $R = 6 \times 10^4$  is evidently higher than the limit of DD2 filter. Thus it is speculated that the failure of CSDA filter beyond  $R = 6 \times 10^4$  may be due to unreasonably accuracy in the

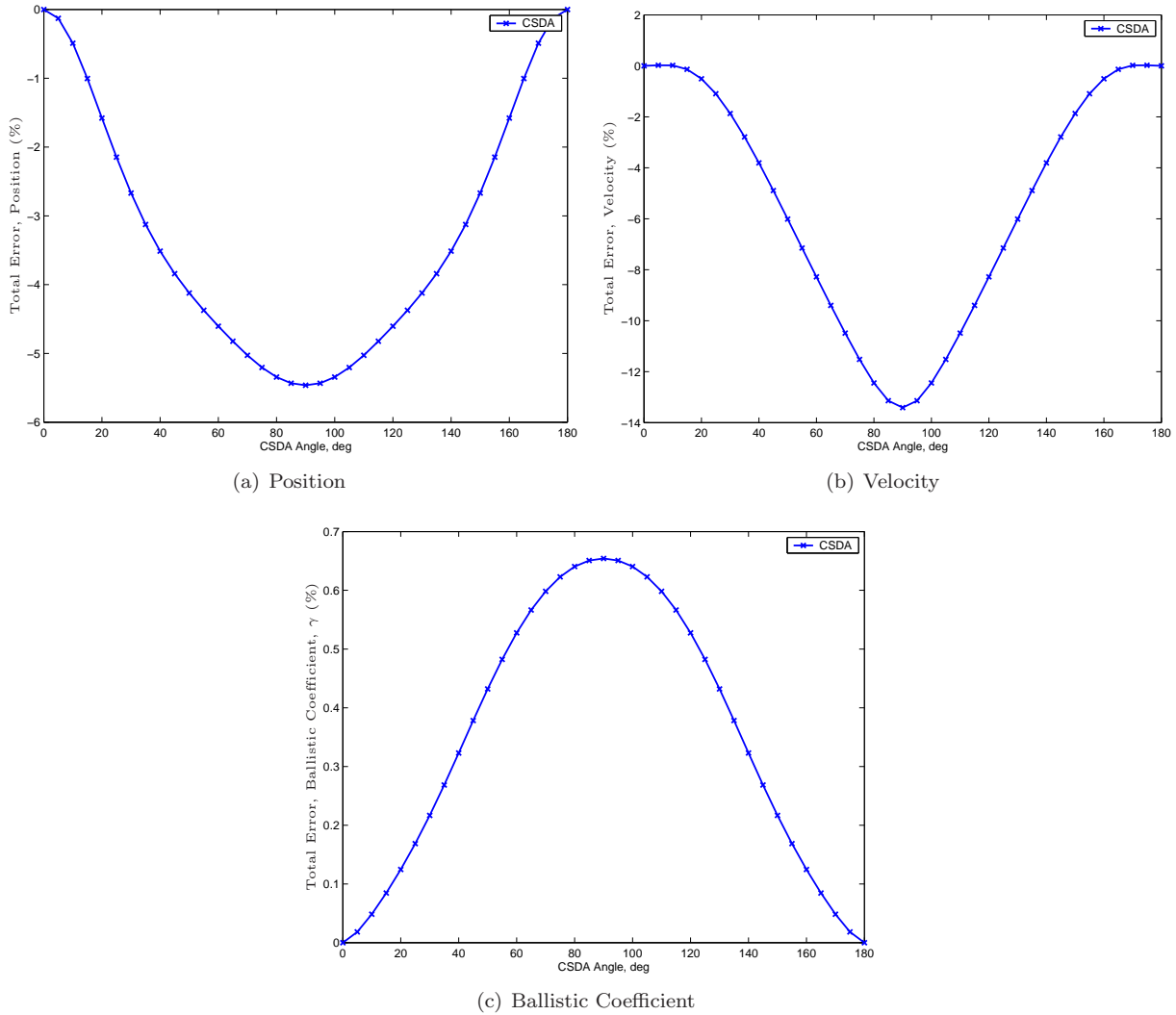


**Figure 7. Percentage of error, varying CSDA angle. Simulations performed with  $h^2 = 2$  and measurement variance  $R = 1 \times 10^4$ .**

ballistic coefficient estimate.

## VIII. Conclusion

In this paper, the first and second-order CSDAs were used in substitution of the first and second-order central divided (finite) difference formulae in the derivation of the DD2 filter. The analysis shows that it is as easy as substituting  $h$  in central divided-difference formulae with one involving a unity magnitude complex number,  $e^{i\theta}h$ . This method generalized the DD2 filter with a complex step size. Assessments were carried out to determine suitable values for  $h^2$  and CSDA angle. Also, the robustness of the CSDA was shown with higher measurement noise. All measures favor the CSDA filter. These proved the robustness of CSDA filter in the face of high nonlinearity. The square-root level filtering of the DD2 and CSDA filters may also provide numerical stability advantages in handling extremely small variables or states with large magnitude differences among them.

## References

<sup>1</sup>Kalman, R. E. and Bucy, R. S., “New Results in Linear Filtering and Prediction Theory,” *Journal of Basic Engineering*, March 1961, pp. 95–108.



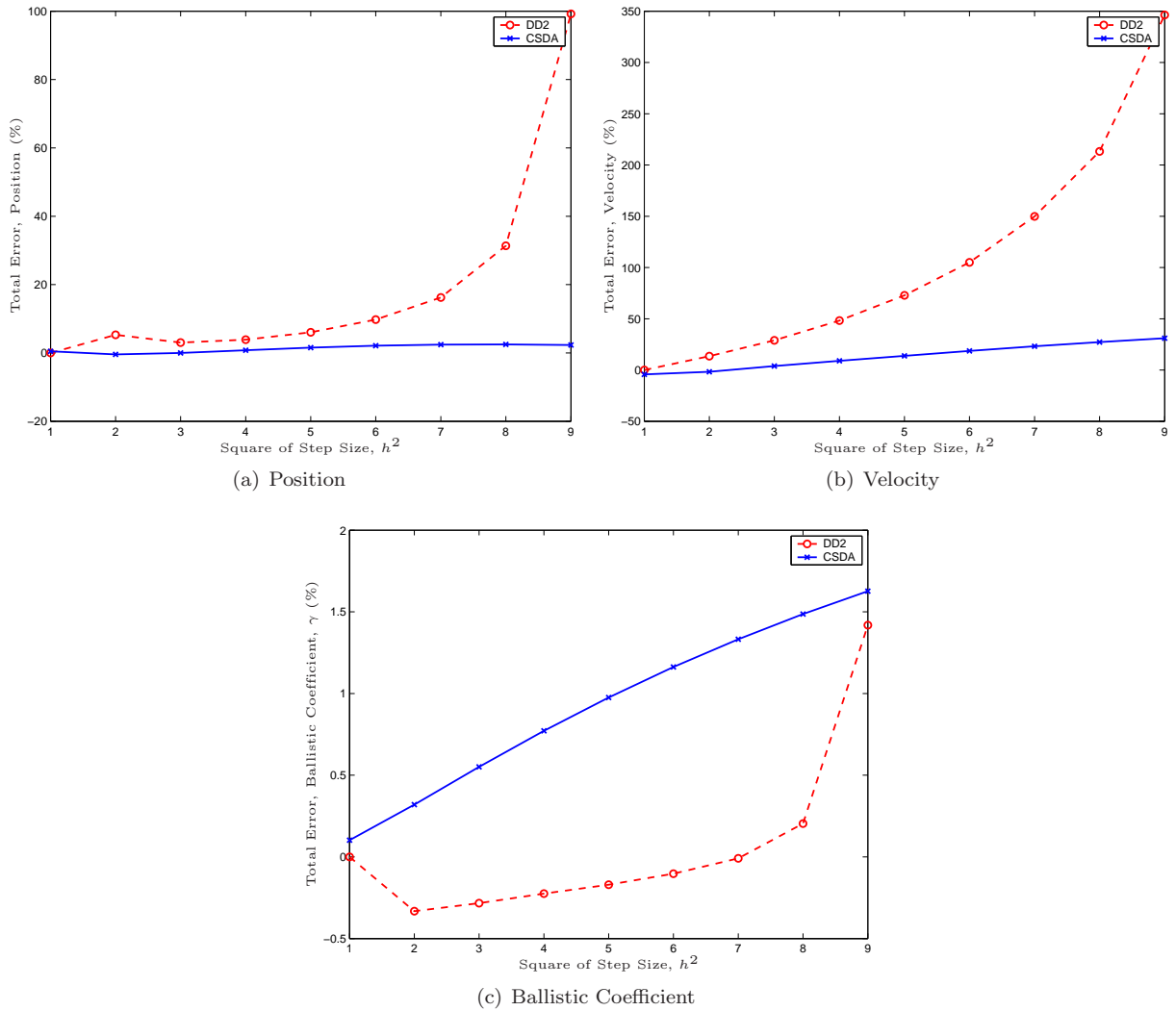


**Figure 8. Percentage of error, varying  $h^2$ . Simulations performed with CSDA angle =  $90^\circ$  and measurement variance  $R = 1 \times 10^4$ .**

<sup>2</sup>Wan, E. and van der Merwe, R., “The Unscented Kalman Filter,” *Kalman Filtering and Neural Networks*, edited by S. Haykin, chap. 7, John Wiley & Sons, New York, NY, 2001.

<sup>3</sup>Gordon, N. J., Salmond, D. J., and Smith, A. F. M., “Novel Approach to Nonlinear/Non-Gaussian Bayesian State Estimation,” *IEE Proceedings, Part F - Communications, Radar and Signal Processing*, Vol. 140, No. 2, Seattle, WA, April 1993, pp. 107–113.

<sup>4</sup>Arulampalam, M. S., Maskell, S., Gordon, N., and Clapp, T., “A Tutorial on Particle Filters for Online Nonlinear/Non-Gaussian Bayesian Tracking,” *IEEE Transactions on Signal Processing*, Vol. 50, No. 2, Feb. 2002, pp. 174–185.

<sup>5</sup>Nørgaard, M., Poulsen, N. K., and Ravn, O., “New Developments in State Estimation for Nonlinear Systems,” *Automatica*, Vol. 36, No. 11, Nov. 2000, pp. 1627–1638.

<sup>6</sup>Lefebvre, T., Bruyninckx, H., and Shutter, J. D., “Kalman Filters for Nonlinear Systems: A Comparison of Performance,” *International Journal of Control*, Vol. 77, No. 7, May 2004, pp. 639–653.

<sup>7</sup>Nørgaard, M., Poulsen, N. K., and Ravn, O., “Advances in Derivative-Free State Estimation for Nonlinear Systems,” Technical Report IMM-REP-1998-15, Department of Mathematical Modelling, DTU, 1998, Revised April 2000.

<sup>8</sup>van der Merwe, R. and Wan, E. A., “Efficient Derivative-Free Kalman Filters for Online Learning,” *Proceedings of European Symposium on Artificial Neural Networks (ESANN)*, Bruges, Belgium, 2001.

<sup>9</sup>Lyness, J. N., “Numerical Algorithms Based on the Theory of Complex Variable,” *Proceedings - A.C.M. National Meeting*, 1967, pp. 125–133.

<sup>10</sup>Greenberg, M. D., *Advanced Engineering Mathematics*, Prentice Hall, Upper Saddle River, New Jersey, 2nd ed., 1998.

<sup>11</sup>Lyness, J. N. and Moler, C. B., “Numerical Differentiation of Analytic Functions,” *SIAM Journal for Numerical Analysis*, Vol. 4, No. 2, June 1967, pp. 202–210.

<sup>12</sup>Martins, J. R. R. A., Sturdza, P., and Alonso, J. J., “The Connection Between the Complex-Step Derivative Approximation and Algorithmic Differentiation,” *AIAA Paper 2001-0921*, Jan. 2001.

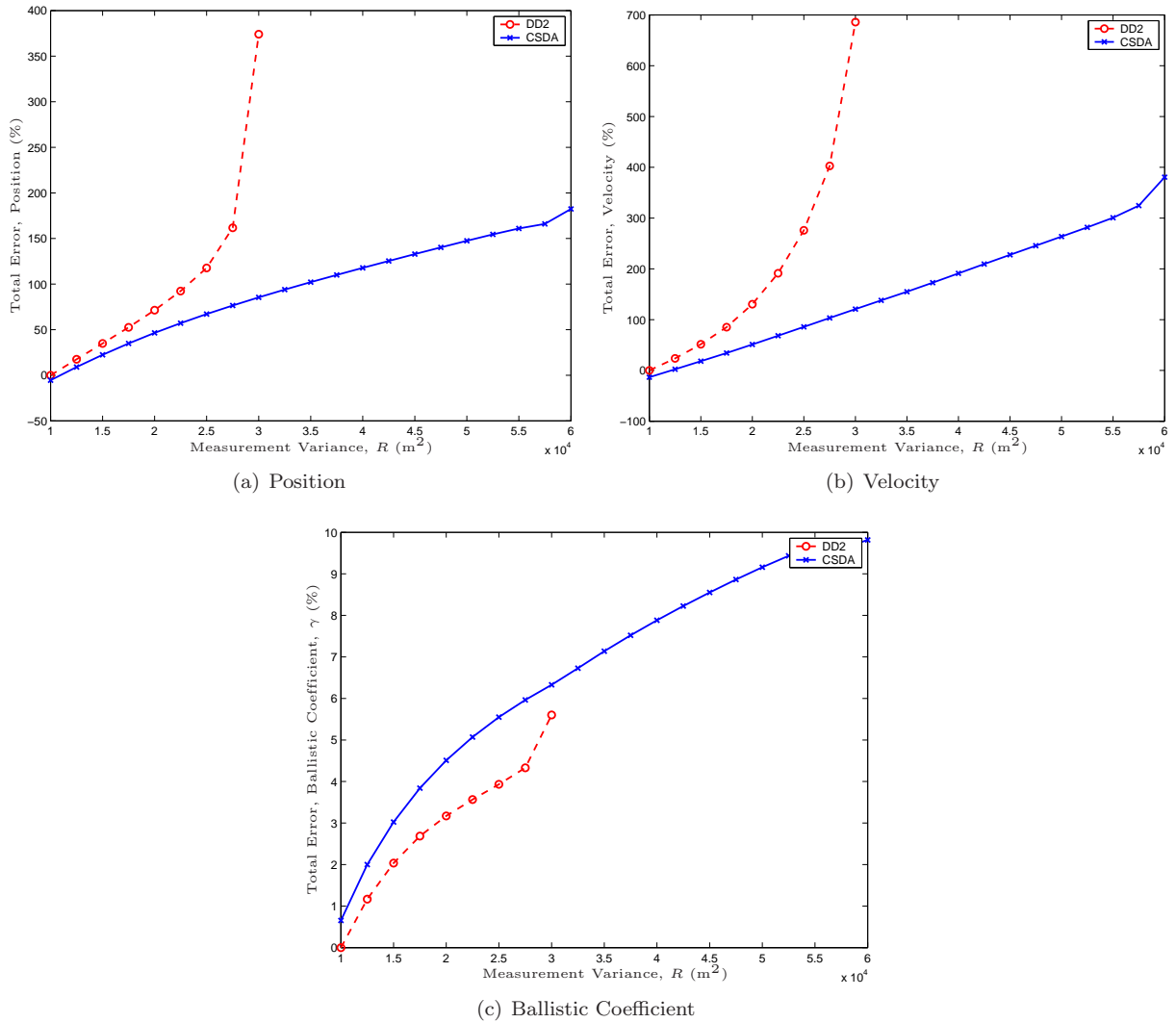


Figure 9. Percentage of error, varying measurement variance. Simulations performed with  $h^2 = 2$  and CSDA angle  $= 90^\circ$ .

<sup>13</sup>Kim, J., Bates, D. G., and Postlethwaite, I., “Nonlinear Robust Performance Analysis using Complex-Step Gradient Approximations,” *Automatica*, Vol. 42, No. 2, 2006, pp. 177–182.

<sup>14</sup>Cerviño, L. I. and Bewley, T. R., “On the extension of the complex-step derivative technique to pseudospectral algorithms,” *Journal of Computational Physics*, Vol. 187, No. 2, 2003, pp. 544–549.

<sup>15</sup>Squire, W. and Trapp, G., “Using Complex Variables to Estimate Derivatives of Real Functions,” *SIAM Review*, Vol. 40, No. 1, Mar. 1998, pp. 110–112.

<sup>16</sup>Martins, J. R. R. A., Sturdza, P., and Alonso, J. J., “The Complex-Step Derivative Approximation,” *ACM Transactions on Mathematical Software*, Vol. 29, No. 3, Sept. 2003, pp. 245–262.

<sup>17</sup>Martins, J. R. R. A., Kroo, I. M., and Alonso, J. J., “An Automated Method for Sensitivity Analysis Using Complex Variables,” *American Institute of Aeronautics and Astronautics*, 2000, AIAA-2000-0689.

<sup>18</sup>Lai, K.-L. and Crassidis, J. L., “Generalizations of the Complex-Step Derivative Approximation,” *AIAA Guidance, Navigation, and Control Conference*, Keystone, CO, Aug. 2006, AIAA-2006-6348.

<sup>19</sup>Fröberg, C.-E., *Introduction to Numerical Analysis*, Addison-Wesley Publishing Company, Reading, MA, second edition ed., 1969.

<sup>20</sup>Athans, M., Wishner, R. P., and Bertolini, A., “Suboptimal State Estimation for Continuous-Time Nonlinear Systems from Discrete Noisy Measurements,” *IEEE Transactions on Automatic Control*, Vol. 13, No. 5, Oct. 1968, pp. 504–514.